UTTAR PRADESH JOURNAL OF ZOOLOGY

43(12): 1-15, 2022
ISSN: 0256-971X (P)

PREPARATION, CHARACTERIZATION AND STUDY OF THE BIOLOGICAL SCREENING OF THE AU (III) COMPLEX WITH NOVEL (AZO -SCHIFF BASE) LIGAND

J. J. EMMAN [a*#], LAYLA ALI MOHAMMED [b] AND KHALIDA KADHIM ABBAS [c]

[a] Faculty of Pharmacy, Pharmaceutical Chemistry Branch, Iraq.
[b] Department of Chemistry, College of Education for Girls, University of Kufa, Iraq.
[c] Clinical Laboratory, Sciences Department, Faculty of Pharmacy, Kufa University, Iraq.

AUTHORS' CONTRIBUTIONS

This work was carried out in collaboration among all authors. Authors JJE, LAM and KKA managed the research. Authors JJE, LAM and KKA done the research and wrote the main manuscript text. Authors JJE, LAM and KKA prepared tables and wrote a part of manuscript text. All authors read and approved the final manuscript.

Article Information

DOI: 10.56557/UPJOZ/2022/v43i123058

Editor(s):
(1) Dr. Telat Yanik, Atatürk University, Turkey.
Reviewers:
(1) Bogdan-Alexandru Hagiu, Alexandru Ioan Cuza University from Iasi, Romania.
(2) S. P. Indra Kumar, Vivekanandha Dental College for Women, India.
(3) Leili mohammadi, Zahedan University of Medical Sciences, Iran.

Received: 07 April 2022
Accepted: 14 June 2022
Published: 20 June 2022

Original Research Article

ABSTRACT

The Aim: Biological studies carried out of new gold complexes after its preparation.
Place and Duration of Study: All preparations were carried out in college of education, chemistry lab between (Jan 2021 to May 2022).
Study Design: New azo –Schiff base ligand 2-amino-3-(2-((3-((2-hydroxy-4-sulfamoylphenyl)imino)-1,5-dimethyl- 2-phenyl- 2,3-dihydro- 1H-pyrazol-4-yl) diazenyl) -1H-imidazol-4-yl)propanoic acid with chelate complexes of Co(II),Ni(II), Cu(II), Zn(II), Cd(II) , Hg(II) and Au(III) were prepared with metal salts in ethanol a solvent in 1:1 ratio (metal : ligand) . The azo-Schiff base ligand has been synthesized from condensation of 2-amino-3- (2-((3-((2 -hydroxy- 4-sulfamoylphenyl) imino)- 1,5-dimethyl -2-phenyl-2,3-dihydro-1H-pyrazol-4-yl)diazenyl)-1H-imidazol-4-yl)propanoic acid with 4-amino-3-hydroxybenzenesulfonamide.
Methodology: The prepared azo Schiff ligand and its metal complexes where checked by different spectral technique as, FT-IR ,C.H.N elemental analyses , Atomic absorption, magnetic moment measurements, molar conductance, UV-vis, ,^{1}H-NMR and mass spectra studies.
Results: The data show that the complexes have the composition of 1:1[M:L] chelates type and octahedral geometry with each of Co(II), Ni(II),Cu(II),Zn(II), Cd(II) and Hg(II) ions, except for Au(III) ion which has square planer geometry. All complexes that non electrolytes and no conductive species but Au(III) complex is 1:2 electrolyte nature. This can support the electrolytic nature of the metal complex.

[#]Ph.D-Student;
**Corresponding author;*

Conclusion: Biological activity studies of the ligand and their metal complexes against several organisms, bacteria Gram positive G(+ve)*staphylococcus aureus and* bacteria Gram negative G (- ve)*Escherichia coli*, In addition to fungi like *Aspergillus Niger*, and *Aspergillus flavus* , are reported. Compounds exhibited the high activity on the growth of all types microorganisms in this study . The results showed the highest inhibitory effect for gold the complex. The effect of biological screening of the gold complex on human colon cancer cell line HT- 29 was investigated. The gold complex was observed to have the highest inhibitory effect.

Keywords: Novel azo- schiff base ligand; 4- amino anti pyrine; biological screening.

1. INTRODUCTION

Amino acids are the basic building elements of proteins, as well as metabolic intermediates and vital components of living organisms [1]. Histidine is an amino acid with an imidazole ring side chain whose charge state is affected by the pH of the surrounding environment. Because of its protonation, which is pH-dependent [2]. Imidazole is an azole heterocycle with two non-adjacent nitrogen atoms that is widely used in natural and manufactured goods. Weak interactions allow imidazole derivatives to bind to a variety of bio receptors and enzymes. It improves the pharmacokinetic features of the pilot molecules, allowing them to be used as an aqueous solubility solution [3]. Azo schiff bases intensify the reaction between azo mixes and the schiff base; these mixes are important because of their wide range of applications, including corrosion prevention and microbe inhibition [4].

2. EXPERIMENTAL AND MATERIALS

All chemicals were supplied by BHD and Sigma Aldrich, Germany, and used without further purification .,The electro-thermal melting point model 9300 was used to measure the melting point of the ligand and its complexes. Elemental analyses were carried out by means of micro analytical unit of 1180 C.H.N elemental analyzer. Electronic spectra were recorded on Shimadzu spectrophotometer double beam model 1700 ultraviolet-visible (UV-Vis) spectrophotometer. . Fourier-transform infrared (FTIR) spectra were recorded in KBr disc on FTIR Shimadzu spectrophotometer model 8400 in wave number 4000- 400/cm. Proton nuclear magnetic resonance (1H-NMR) and carbon nuclear magnetic resonance (13C-NMR) spectra in ppm unit were operating in dimethyl sulfoxide-d6 (DMSO-d6) as solvent using (Bruker) Ultra Shield 3000 MHz, Switzerland). And mass spectra were recorded on AB Sciex 3200 QTRAP LC/ MS/MS (mass range m/z 5-2000 quad mode and 50- 1700 linear ion trap mode). Magnetic susceptibility measurements were carried out on a balance magnetic MSB-MKI using faraday method. The diamagnetic corrections were made by Pascal's constants.

2.1 Azo-Schiff Ligand Synthesis

1- In the first step, 0.01mol of 4-aminoantipyrine was dissolved in solution of 3ml HCl and 30ml distilled water. After cooling in an ice bath with stirring for 15 minutes, the mixture was treated with Sodium nitrite solution NaNO2 (0.01mol) was added drop by drop with continuous stirring. After allowing the solution to settle for 30 minutes to complete the dialysis process .The cooled amino acid (histidine 0.01mol) solution in an alkaline medium (NaOH 10%) added of the solution was observed to be colored red. Following the completion of the addition, a red precipitate was allowed to settle before being filtered and washed several times with distilled water. It was re-crystallized using hot absolute ethanol after drying. The product percentage was (90%) and the melting point was (215-217)^{0}C. The reaction equations are depicted in Scheme 1.

2- (0.01mol) from azo compound was dissolved in (50 ml) of absolute ethanol, and (0.01mol) of -4-amino-3-hydroxybenzene sulfonamide was added and dissolved in 25 ml of absolute ethyl alcohol, before 3 drops of acid were added. the reaction mixture and refluxed with stirring for 45 h. With the precipitate product collected by filtering off, the resulting solution was evaporated to half volume, purified by crystallization from hot ethanol, and dried over anhydrous CaCl2, and the yield percentage (96%) and melting point (162-163 ^{0}C) were calculated. The method of preparation is depicted in Scheme 1.

2.2 Preparation of Metal Complexes

The metal complexes were prepared by mixing 25 mL ethanol solution of, CoCl2 6H2O, NiCl2 6H2O, CuCl2 2H2O, ZnCl2, CdCl2 2H2O, HgCl2 2H2O, NaAuCl4 H2O with 25 mL ethanol solution of azo Schiff-base ligand in 1 : 1 (metal : ligand) ratio. The resulting mixture was refluxed for 1 h. The product was isolated after the volume was reduced by evaporation. It was filtered off, washed with ethanol and dried under vacuum. The complexes obtained are listed in Table 1.

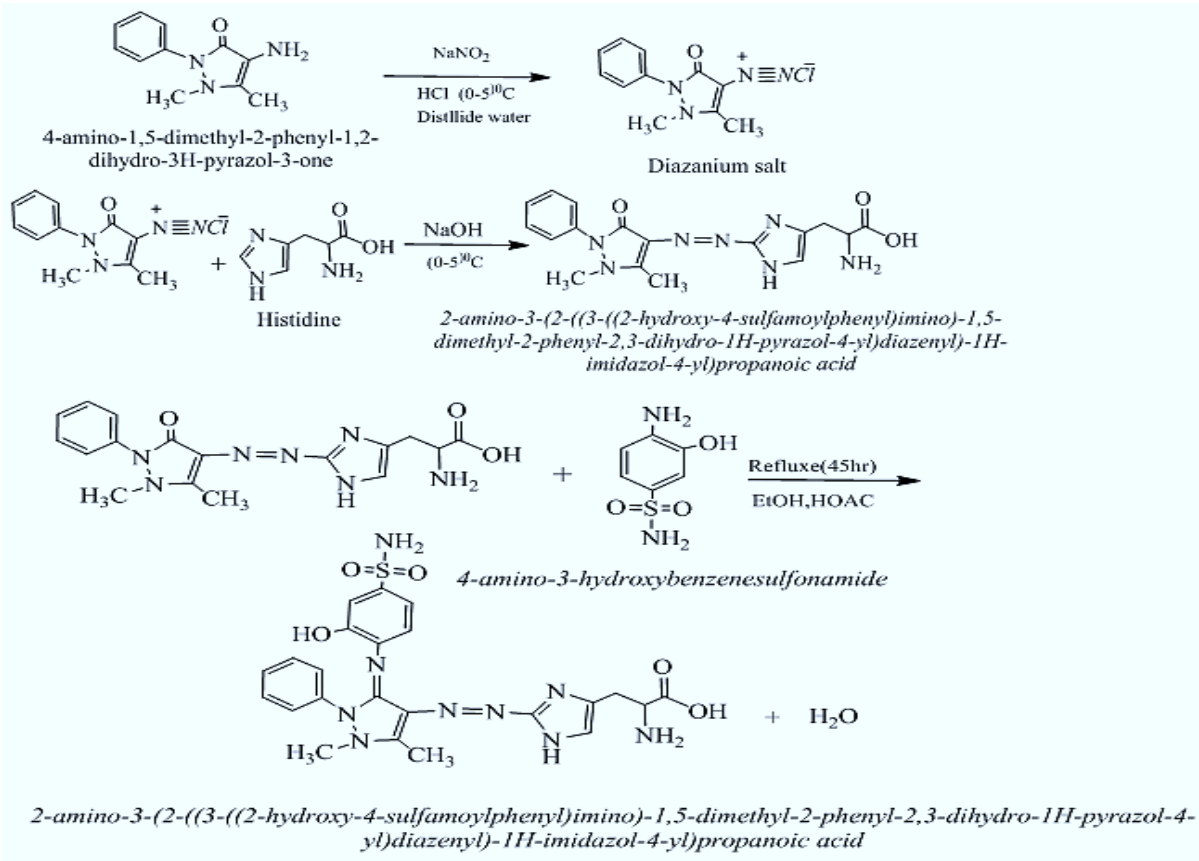

Scheme1. Preparation of ligand of the azo -schiff

Table 1. Shows the percentages and some physical properties of ligand and its metal complexes

N_O.	Cheimiecal formula	M .wt	m.p. ^OC	Color	Yeiled%
1-	L: $C_{23}H_{25}N_9O_5S$	539.57	162-163	Red	96%
2-	[Co LCl H_2O]	650.96	>300	Purple	92%
3-	[Ni L Cl H_2O]	650.72	>300	Purple	95%
4-	[Cu L Cl H_2O]	655.57	239-241	Dark brown	89%
5-	[Zn L Cl H_2O]	657.41	174-176	Dark brown	90%
6-	[Cd L Cl H_2O]	704.44	178-180	Purple	93%
7-	[Hg L Cl H_2O]	792.62	143-145	Purple	89%
8-	[Au L] Cl_2	806.43	210-212	Purple	95%

2.3 Biological Part

2.3.1 Determination of antimicrobial activity

The purpose of the screening program is to provide antimicrobial efficiencies of the investigated compounds. The prepared compounds were tested against some Fungi and bacteria to provide the minimum inhibitory concentration (MIC) for each compound. The antimicrobial activities of the investigated compound were tested against the bacterial species *staphylococcus aureus*(+ve), *Escherichia coli*(-ve), ,and fungal species *Aspergillus Niger*, and *Aspergillus flavus* by the well diffusion method for preparation of plates and inoculation , 1.0 ml of in ocular were added to 50 ml of agar media(50c0) and mixed . The agar was poured into (120 mm) petri dishes and allowed to cool to room temperature. Wells (6mm in diameter) were cut in the agar plates using proper sterile tubes. Then, Fill wells were filled up to the surface of agar with 0.1ml of the test compounds dissolved in ethanol. The plates were left, on leveled surface, incubated for 24 hats 30^0C for bacteria and 48h for fungi and the diameter of the inhibition zones were read. The results were compared with a similar run of standards of antibacterial and anti-fungal drugs that showed no microbial growth by visual observation of the

complexes was determined by serial dilution technique

2.4 Cytotoxicity Assay

All vials were tightly closed, affixed with name and date and kept in an incubator at 37°C. The vials were checked after (2-3)days. To ensure that it is not turbid and is not exposed to bacterial growth, and after examination, it is transferred to the refrigerator for storage until use.

The anticancer activity of gold complexes with ligand in against HT-29 and vero was evaluated by MTT assay, (3-(4,5-Dimethylthiazol-2-yl)-2,5-diphenyltetrazolium bromide) MTT assay. Chromatography is an established method for determining cell viability and cytotoxicity studies. This assay is based on the cleavage of yellow tetrazolium salt, MTT, to form a soluble blue formazan product by mitochondrial enzymes (in growth cells), and the amount of formazan produced is directly proportional to the number of live cells, not dead cells, present during MTT exposure. Since the MTT test is fast, easy and economical, In this method, it has become a very popular method for quantifying live cells. Cell lines were cultured on 96 well plates at a concentration of 1.0 x l05 cells/ml. After being kept in incubation at 37°C for 48 hrs and once the fused monolayer of HT-29 VERRO cells is completed (80% - 100%), the prepared concentrations are added (1 µg/ml,10 µg/ml, 100) µg/ml, 250 µg/ml, 500 µg/ml and 1000 µg/ml) of [AuL]Cl_2 and 5FU to growth cells with a final volume of 100 µl in each hole except for the untreated (form-free) control cells The plank and tripled ie three holes for each concentration. The maximum concentration of DMSO (0.01%) was used as a negative control. After 48 hrs incubation at 37°C in 5% CO_2, the well plates were transferred to a biosafety cabinet with a sterile environment to avoid any contamination. All plate medium used was discarded. . The well was washed with PBS solution to remove any residual ligand -gold complex and 5FU solutions that might interact with MTT reagents, then 100 µl of retaining medium was added to all pits containing the treated drug. Cells, drugs, untreated cells and empty pits. Then MTT reagent (20 µl) was added to each plate. After 4 hrs of incubation at 5% CO_2, 37°C, % formazan crystals were observed as a mitochondrial enzymatic process of unaffected organelles were disrupted. Formazan was dissolved by adding 100 µl of solubilization solution Dilute DMSO (1:1 in isopropanol) was formed on each hole including the blank. The absorbance was read at 490 nm at a reference wavelength of 630 nm by an ELASIS READER. The measurement mechanism of the MTT test is reported in Several sources The average Blank absorption was subtracted from other samples and the pit absorption was adjusted. The same method was performed for VERRO normal cells.

3. RESULTS AND DISCUSSION

3.1 Mass Spectrometry

The mass spectra of synthesized azo Schiff-base ligand and its Zn(II) complex were recorded at room temperature. The obtained molecular ion peaks confirmed the proposed formulae for the synthesized compounds. The mass spectrum of the ligand shows the molecular ion peak at m/z 537 for the compound $C_{23}H_{25}N_9O_5S$, confirming the proposed formula for the synthesized compound. Also The mass spectrum of the Zn(II) complex exhibited the molecular ion peak at m/z 657 for the molecular formula Zn(C23H23N9O5S), which was consistent with the molecular weight of the Zn(II) complex and in good agreement with their formula as expressed from micro analytical data. The mass spectral data fragmentation of the ligand and Zn(II)-complex are shown in Scheme 2, 3, and Fig. 1.

3.2 ^{1}HNMR Spectra

The 1H-NMR spectrum of the ligand showed the following signals: Phenyl multiples at 6.8-7.5ppm, =C-CH3 at 2.02 ppm, -N-CH3 at 3.2 ppm**,** ($CHNH_2$) of the histidine at (4.1) ppm [5], NH imidazole ring at 12.9 [6] ppm. The sign of the solvent protons appeared at (2.5) ppm and -OH at 10.2 ppm [7] This peak was lost in the spectra of complexes indicated that the –OH proton contribute to the complexity. There was no appreciable change in all other signals in the complexes, as shown Fig. 2.

3.3 Infrared Spectra

"The FTIR spectra provided valuable information regarding the nature of the functional group attached to the metal atom. The most important infrared spectral bands that provided conclusive structural evidence for the coordination of the ligand to the central metal ions are given in Table 4. The FTIR spectrum of the ligand showed characteristic bands at 1622 and 1492/cm due to the C=N and N=N functional groups, respectively" [8-9]. "The IR spectra of the ligand exhibited appropriate shifts due to the formation of all complexes prepared in this study. The C=N and N=N bands in the free ligand shifted for the complexes. The reduction in bond order, upon complexion, could be attributed to the delocalization of metal electron density (t_2g) to the -system of the ligand. These shifts confirmed the coordination of the ligand via the nitrogen of azo methine and the azo

groups to metal ions. The absorption band in free ligand observed at 3350/cm was attributed to the υ(OH) of hydroxyl group. This band changed in the spectra of their complexes, which suggested that the hydroxyl group was taking part in coordination" [10]. As for the group stretch beam (C=N), for the amino acid's imidazole ring Histidine appeared in the ligand at frequency (1589) cm^{-1}, and the spectrum of metal complexes showed a shift towards lower frequencies as well as a change in shape and intensity, indicating their participation in the coordination process [11]. Two sharply intense stretching bands were observed in the ligand's spectrum at frequencies (1149, 1319) cm^{-1} [12], which correspond to the symmetrical and asymmetric vibrational frequencies of the sulfonyl group (O=S=O), as there was no change in this band in the spectra of the metal complexes. The infrared spectrum of the metal complexes also revealed new absorption bands associated with the ν(M–O) and (ν(M–N) [13,14] bonds at positions (507-540) and (420-476) cm^{-1}, respectively. The stretching beams of the active groups belonging to the ligand and its metal complexes are shown in Table 2.

3.4 Analysis of Elements of Biological Compounds

The preparatory analysis data for the 1:1 ratio pools [M:L] revealed that the theoretical values agreed well with the existing data, as shown in Table 3. TLC technology and C, H, N elemental analysis were used to determine the purity of the new ligand.

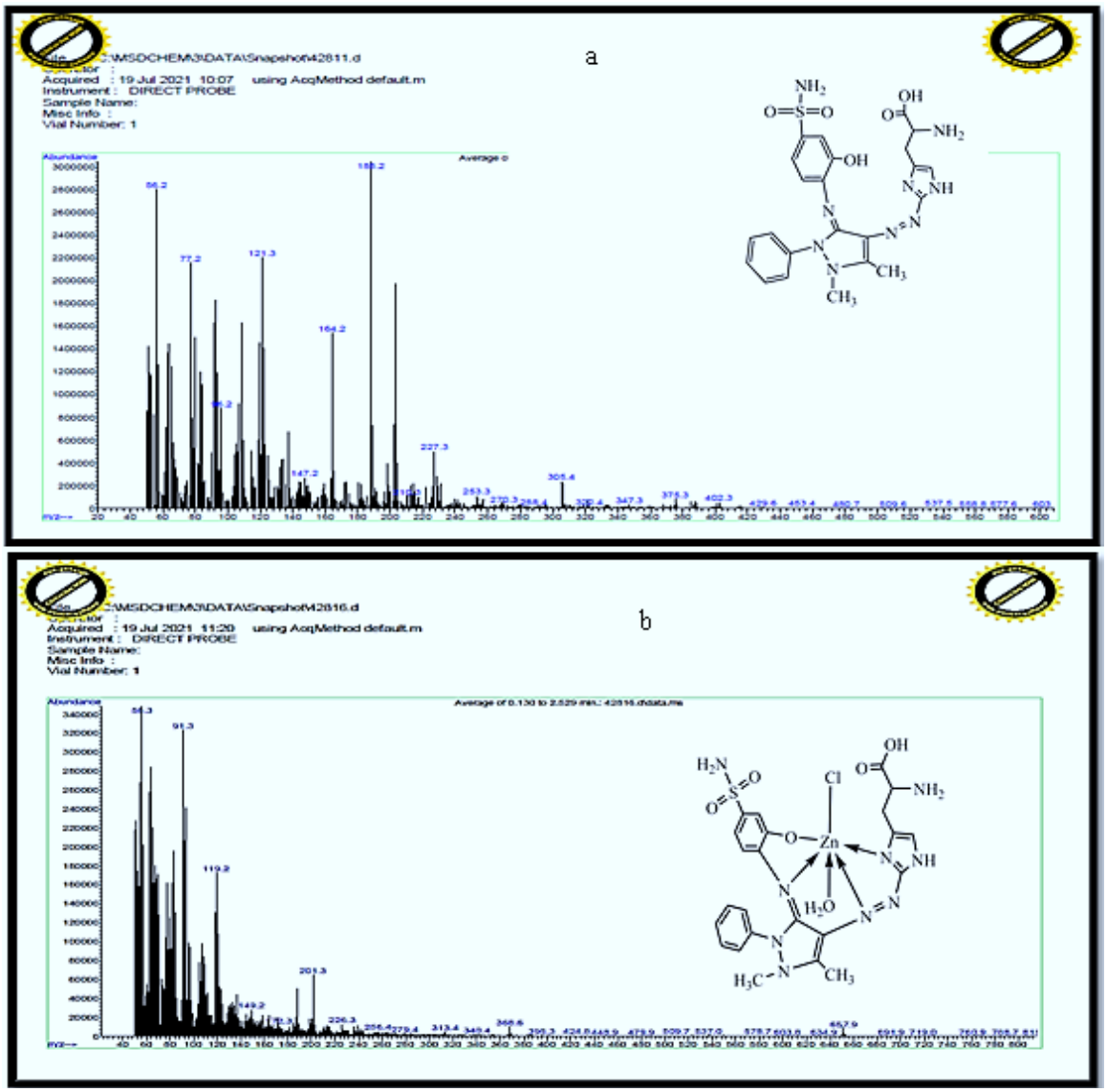

Fig. 1. a and b show Mass spectrum of the ligand and Zn(II) respectively

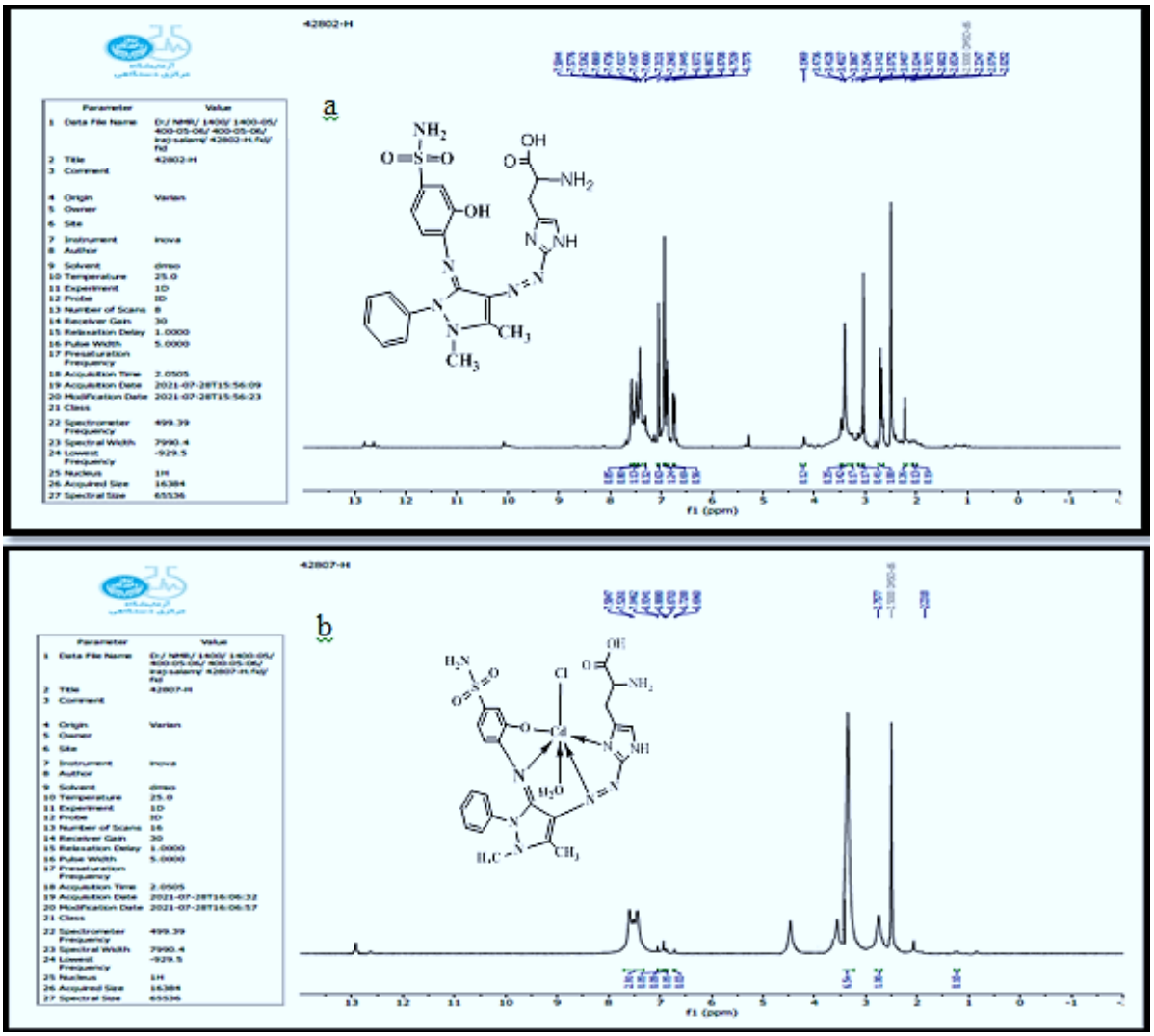

Fig. 2. a and b show the ^{1}HNMR spectrum of the ligand and Cd-complex

3.5 Electronic Spectra

The UV-Visible spectra were obtained in an ethanol solution (10^{-5}M). The spectrum of a novel azo-schiff base ligand shows three bands: the first at 245nm to ($\pi-\pi^*$) transition of histidine's heterocyclic ring [15], the second at 386nm to ($\pi-\pi^*$) transition of schiff base group [16], and the third at 489nm to ($n-\pi^*$) electronic transmission of (-N=N-) [17]. during metal coordination [18]. Table 6 describes the electronic transmission of (Co,Ni,Cu, and Au)(III) complexes. The electronic spectrum of Co(II) complex shows three bands at 981 nm (10193 cm^{-1}), 890 nm (11235 cm^{-1}) and 575 nm (17391 cm^{-1}). These three bands correspond to $^{4}T_1g(F)\rightarrow {}^{4}T_2g(F)$=v1, $^{4}T_1g(F)\rightarrow {}^{4}A_2g(F)$ = v2, and $^{4}T_1g(F)\rightarrow {}^{4}T_1g(p)$ = v3 transitions, respectively [19]. Three absorption bands were observed in the electronic spectrum of Ni(II) complex, at 980 nm (10204 cm^{-1}), 888 nm (11261 cm^{-1}) and 577 nm (17331 cm^{-1}). These bands can be assigned to transitions $^{3}A_2g\rightarrow {}^{3}T_2g$ (F) =v(1), $^{3}A_2g\rightarrow {}^{3}T_1g(F)$=v2 and $^{3}A2g\rightarrow {}^{3}T_1g(p)$ =v3, respectively. The spectrum is similar to what has been reported for octahedral complexes [20]. The electronic spectrum of the Cu(II) complex included bands at 974nm (10224 cm^{-1}), 847nm (11806 cm^{-1}) and 567nm (17574 cm^{-1}). These bands can be assigned to $^{2}B1g\rightarrow {}^{2}A_1g$=V1, $^{2}B_1g\rightarrow {}^{2}B_1g$=V2, and $^{2}B_1g\rightarrow {}^{2}Eg$ = V3 transitions, respectively. These results suggested a distorted octahedral geometry surrounding the Cu(II) ion [21]. While (Zn,Cd, and Hg) (II) complexes appeared Charge Transfer (ML,CT), because they are rich in electrons (nd^{10}) [22]. The electronic spectrum of Au(III) complex shows one band at 500 nm (20000 cm^{-1}) [23]. The electronic transmission of metal complexes is depicted in the Table 4.

Table 2. Values of infrared frequencies (cm^{-1}) for the ligand and its chelating complex

Compound	**(O-H) Phenl**	**υ(O-H) COOH**	**NH_2**	**υ(C=N) Schiff**	**(C=N) imidazole**	**υ(N=N)**	**υ(SO_2)**	**(M-O)**	**(M-N)**	**Other bound**
L: $C_{23}H_{25}N_9O_5S$	3350		3280-3334	1622	1589	1492-1413	1319-1149	……	……	……
[Co LCl H_2O]	……	3500	3045-3143	1631	1539	1406	1325-1155		514	
[Ni L Cl H_2O]	……	3500	3282-3390	1610	1581	1408	1321-1151		513	
[Cu L Cl H_2O]	……	3500	3356-3390	1604	1577	1408w	1315-1149		530	
[Zn L Cl H_2O]	……	3500	3288-3334	1612	1510	1406w	1315-1149	453w	511	3334 935
[Cd L Cl H_2O]	……	3500	3271-3332	1625	1587	1458-1411w	1321-1147	476w	507	3421 931
[Hg L Cl H_2O]	……	3500	3292-3333	1616	1510	1406w	1313-1143	459w	511	3400 939
[Au L] Cl_2	……	3600	3242-3300	1629	1589	1487-1415w	1311-1149	432w	540	……

Table 3. Results of the micro-analysis of the elements for ligand and complexes

No	Formula	M.Wt	Found (Calc.)%			
			C%	H%	N%	M%
1	L : $C_{23}H_{24}N_9O_5S$	539.57	51.20 (51.33)	4.67 (4.53)	23.36 (23.45)	.....
2	[Co($C_{23}H_{25}N_9O_5S$) H_2O Cl]	650.96	42.44 (42.60)	4.03 (4.21)	19.37 (19.11)	9.05 (8.89)
3	[Ni($C_{23}H_{24}N_9O_5S$) H_2O Cl]	650.72	42.45 (42.22)	4.03 (4.15)	19.37 (19.53)	9.02 (9.19)
4	[Cu ($C_{23}H_{24}N_9O_5S$) H_2O Cl]	655.57	42.14 (42.00)	4.00 (4.20)	19.23 (19.23)	9.69 9.45)(
5	[Zn($C_{23}H_{24}N_9O_5S$) H_2O Cl]	657.41	42.02 (42.21)	3.99 (3.76)	19.17 (19.03)	9.95 (9.83)
6	[Cd($C_{23}H_{24}N_9O_5S$) H_2O Cl]	704.44	39.22 (39.00)	3.72 (3.90)	17.90 (17.70)	15.96 (15.73)
7	[Hg($C_{23}H_{24}N_9O_5S$) H_2O Cl]	792.62	34.85 (34.96)	3.31 (34.08)	15.90 (15.81)	25.31 (25.54)
8	[Au($C_{23}H_{24}N_9O_5S$)] Cl_2	806.43	34.26 (34.44)	3.00 (3.37)	15.63 (15.35)	24.42 (24.29)

Table 4. The electronic transmission of metal complexes

Compounds	λ (nm)	ύ (cm^{-1})	Transitions	Geometry	Hybridization
L: $C_{23}H_{25}N_9O_5S$	245	40816	π →π*	……	……
	368	27173	π →π*		
	489	20449	n →π*		
[Co LCl H_2O]	981	10193	$^4T_1g_{(F)} \rightarrow {}^4T_2g_{(F)} = \nu_2$	Octahedral	Sp^3d^2
	890	11235	$^4T_1g_{(F)} \rightarrow {}^4A_2g_{(F)} = \nu_2$		
	575	17391	$^4T_1g_{(F)} \rightarrow {}^4T_1g_{(p)} = \nu_3$		
[Ni L Cl H_2O]	980	10204	$^3A_2g \rightarrow {}^3T_2g_{(F)} = \upsilon 1$	Octahedral	Sp^3d^2
	888	11261	$^3A_2g \rightarrow {}^3T_1g_{(F)} = \upsilon 2$		
	577	17331	$^3A_2g \rightarrow {}^3T_1g_{(p)} = \upsilon 3$		
[Cu L Cl H_2O]	974	10224	$^2B_1g \rightarrow {}^2A_1g = \upsilon 1$	Octahedral	Sp^3d^2
	847	11806	$^2B_1g \rightarrow {}^2B_1g = \upsilon 2$		
	569	17574	$^2B_1g \rightarrow {}^2Eg = \upsilon 3$		
[Zn L Cl H_2O]	570	17543	$d\pi(Zn)^{+2} \rightarrow \pi^*(L)$	Octahedral	Sp^3d^2
[Cd L Cl H_2O]	579	17271	$d\pi(Cd)^{+2} \rightarrow \pi^*(L)$	Octahedral	Sp^3d^2
[Hg L Cl H_2O]	548	18248	Intra–ligand $d\pi(Hg)^{+2} \rightarrow \pi^*(L)$	Octahedral	
[Au L]Cl_2	500	20000	$^1A_1g \rightarrow {}^1B_1g$	square planer	dsp^2

3.6 Magnetic Measurements

"The magnetic moment of the Co(II) complex is 3.31 B.M, which is consistent with the reported value for octahedral Co(II) complexes" [24]. "The magnetic moment value of the Ni(II) complex is 2.82 B.M" [17] "indicating an octahedral environment". "The magnetic moment value of the Cu(II) complex is 1.75 B.M, which is consistent with distorted octahedral geometry" [25]. "The complexes Zn(II),Cd(II),Hg(II), and Au(III) are diamagnetic, and according to empirical formulae, an octahedral geometry is proposed, except for the Au(III) complex, which suggests a square planar geometry" [26]. We can deduce the probable structures of the complexes from the above results.

3.7 Conductivity Measurement

"Molar conductance (Λm) measurements of the metal complexes Table 5. All chelate complexes prepared in this work showed conductivity values ranged between (4. 1-10.3) S. $mol^{-1}.cm^2$, in the DMF at room temperature, all these complexes are non-electrolytic species" [27] compared with the high values of conductivity of Au(III) complex [28]. This could support the electrolytic nature of the metal complex.

Table 5. The values of molar conductivity and magnetic susceptibility for ligand complexes

Compounds	μ_{eff} (B.M)	Conductivity $S.mol^{-1}. Cm^2$
[Co L_3Cl H_2O]	3.31	10.2
[Ni L_3 Cl H_2O]	2.82	10.3
[Cu L_3 Cl H_2O]	1.75	8.1
[Zn L_3 Cl H_2O]	Dia	7.2
[Cd L_3 Cl H_2O]	Dia	7.6
[Hg L_3 Cl H_2O]	Dia	4.1
[Au L_3]Cl_2	Dia	85.2

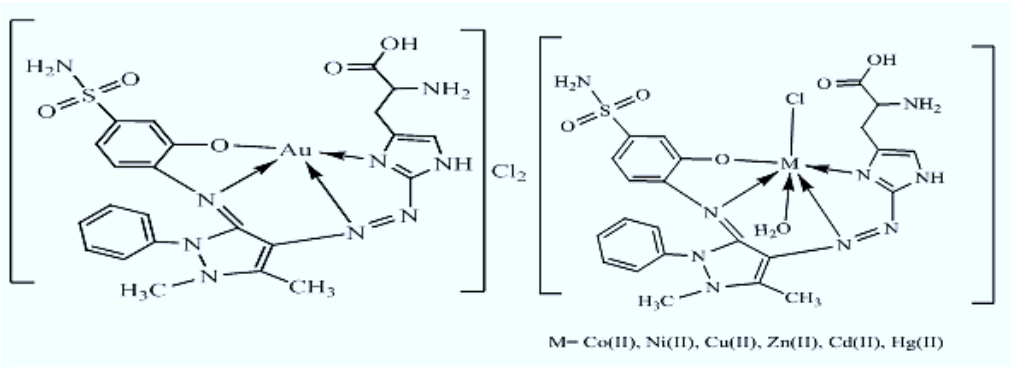

Fig. 3. The proposed structural formula of the metal chelate complexes

3.8 The Influence of Gold Complex on the Growth of HT-29 Colon Cancer Cell Lines

The lowest percentage of cell growth inhibition after treatment was 27.7 percent and 30.9 percent, respectively, and the highest percentage of inhibition after treatment was 97.0 percent and 98.0 percent for HT-29 colon cancer cell lines and normal cells Straight. Ordinary cells were compared to cancer cells to determine the extent to which it can be used as a drug against this type of cancer. In comparison to the cells of the normal line, the half inhibitory concentration was (59.04 g/ml) (VERRO).), as concentrations up to 1000 were approved to be (IC50) logical, and this is a good result, that is, the [AuL]Cl2 complex kills colon cancer cells HT-29, but has almost no effect on normal cells (VERRO), because it requires a very high concentration before half of them are killed, and this result is very important in using the mentioned gold complex as a selective treatment at a very high rate for the treatment of HT-29 colon cancer. As illustrated in the Tables 6-8 and Figs. 4, 5.

3.9 The Effect of the Drug Fluorouracil on the Growth of Colon Cancer Cell Lines HT-29 as well as Normal Cells (VERRO)

When the gold complex was compared to the therapeutic drug for colon cancer (fluorouracil), it was discovered that increasing the drug concentration increases the percentage of cell growth inhibition for cancerous lines. For cell lines, the lowest percentage of cell growth was found at a concentration of 1 g/ml and the highest percentage of inhibition was found at a concentration of 1000 g/ml. As shown in Tables 7, 8 and Figs. 6-10. This result is similar to the gold complex results in that increasing the concentration of gold complex (III) increases the rate of cell growth inhibition for cancerous lines drug and the gold complex (III). (This is dose-dependent.)

Table 6. The effect of the [AuL]Cl_2 complex on the cells of the colon cancer cell line HT-29 and its comparison with the normal cell line VERRO for the same concentrations using MTT test for 24 hours at a temperature of 370C

(x) =Conc. µg / ml	1	10	100	250	500	1000
Log x	0	1	2	2.4	2.7	3
Inhibition % Colon Cell Line	27.7	45.2	63.9	77.1	86.1	97.0
Inhibition % RET Cell Line	30.9	28.4	89.7	95.3	98.2	98.9
Colon HT-29 Cell Line IC50=59.04 *µg/ml*			VERRO Cell Line IC50 =51.23µg/ml			

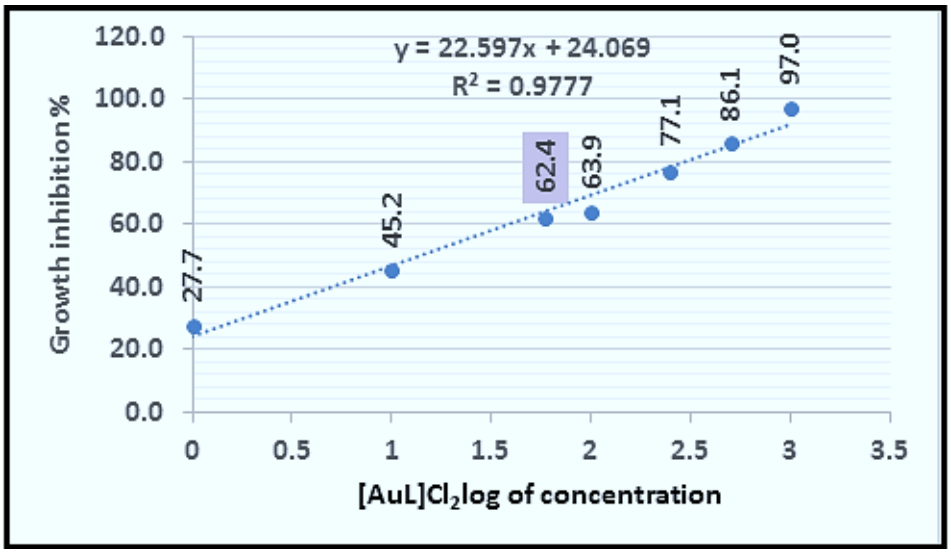

Fig. 4. Percentage of inhibition in HT-29 colon cancer line cells vs. logarithm of complex $[AuL]Cl_2$ concentration

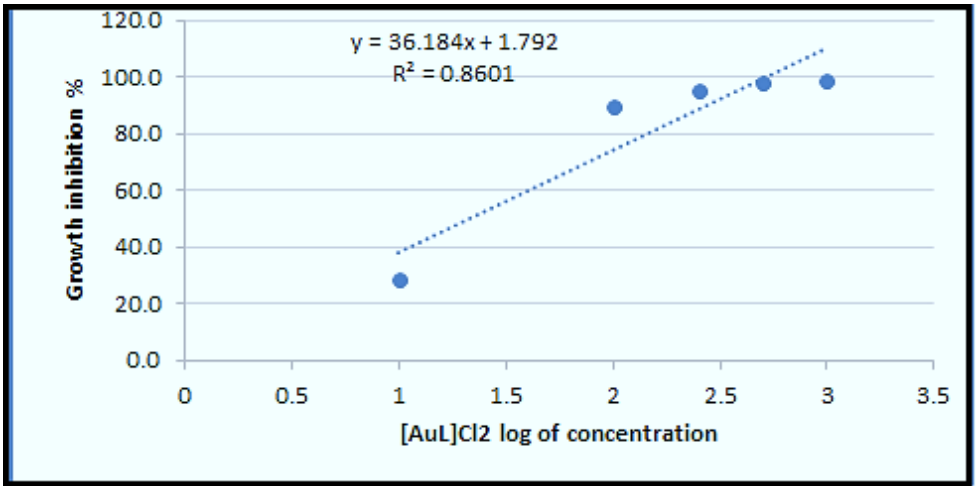

Fig. 5. Percentage of inhibition in cells of the normal line VERRO against the logarithm of the concentration of the complex $[AuL]Cl_2$ when concentrations up to 1000 are adopted

Table 7. The effect of the drug Fluorouracil on the cells of the colon cancer cell line HT-29 for the same concentrations using the M TT test for a period of 24 hours at a temperature of 370C

(x) =Conc μg / ml	1	10	100	250	500	1000
Log x	0	1	2	2.4	2.7	3.0
Inhibition %	51.8	57.0	70.7	65.7	68.5	73.7
Y=62.75,	logIC50=1.5869,			IC50=38.63		

Table 8. Effect of fluorouracil on VERRO normal line cells - concentrations using MTT Test for a Period of 24 hours at a temperature of 37 C

(x) =Conc μg / ml	1	10	100	250	500	1000
Log x	0	1	2	2.4	2.7	3.0
Inhibition %	16.8	34.8	62.4	60.1	60.9	63.9
	Y=40.35, logIC50=1.273, IC50=18.753					

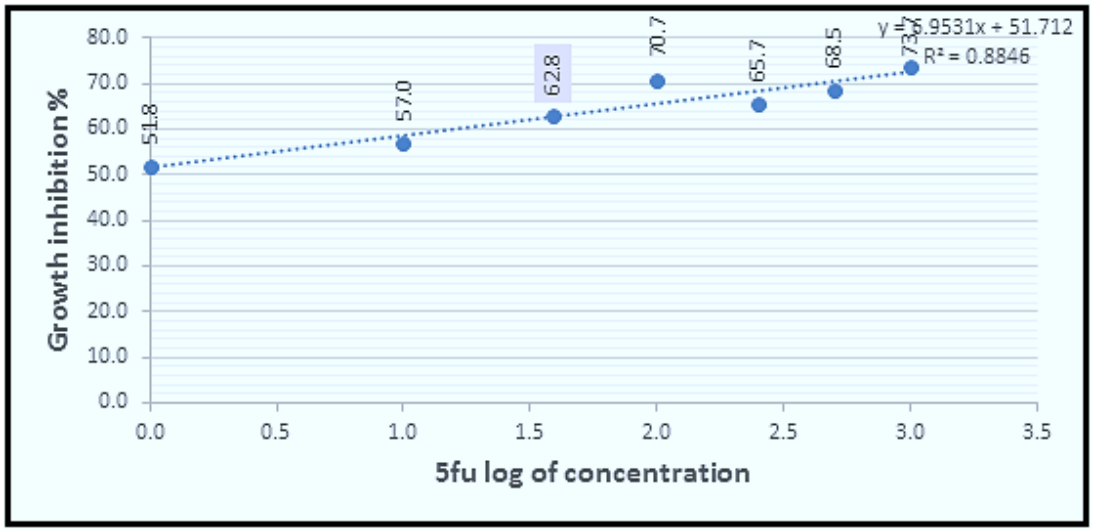

Fig. 6. Percentage of inhibition in cells of the colon cancer line HT-29 vs. logarithm of the concentration of the drug fluorouracil

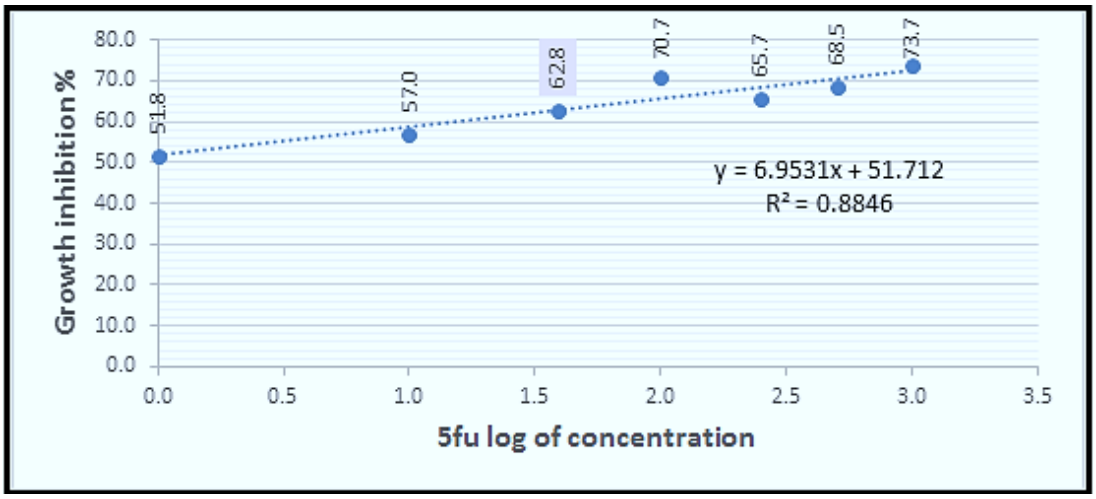

Fig. 7. Percentage of inhibition in cells of the normal line VERRO vs. logarithm of the concentration of the drug fluorouracil

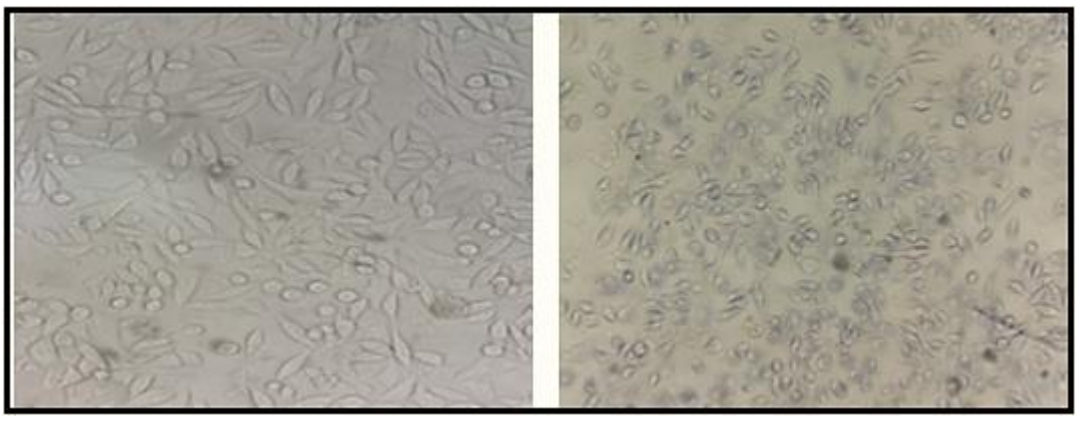

Fig. 8. Untreated cancer cells without MTT and cancer cells untreated with MTT

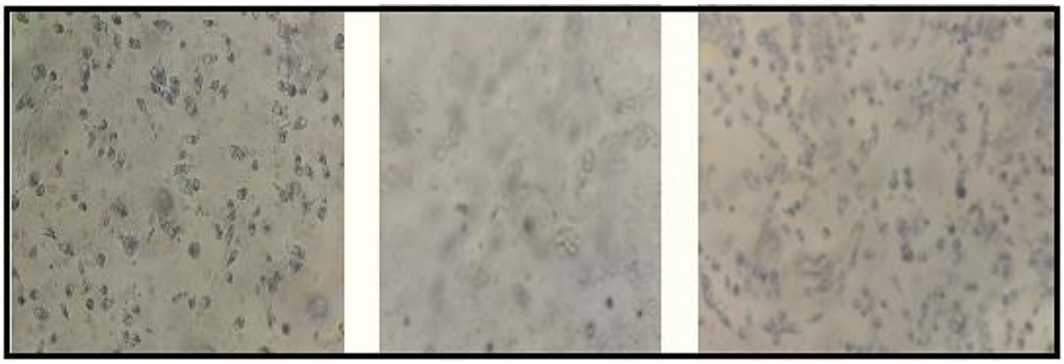

Fig. 9. Cancer cells treated with [AuL]Cl2 at different concentrations after adding MTT

3.10 Investigation of the Antifungal Activity of Gold Complex Prepared with the Ligand

Pathogenic fungi (Aspergillus flavus and Aspergillus neger) that cause many common diseases in humans, animals, and plants were chosen. Under the same conditions, three ppm (250,500,1000) concentrations were used in DMSO solvent. As illustrated in Fig. 10, these compounds have demonstrated very high efficacy in inhibiting and limiting the growth of these types of fungi.

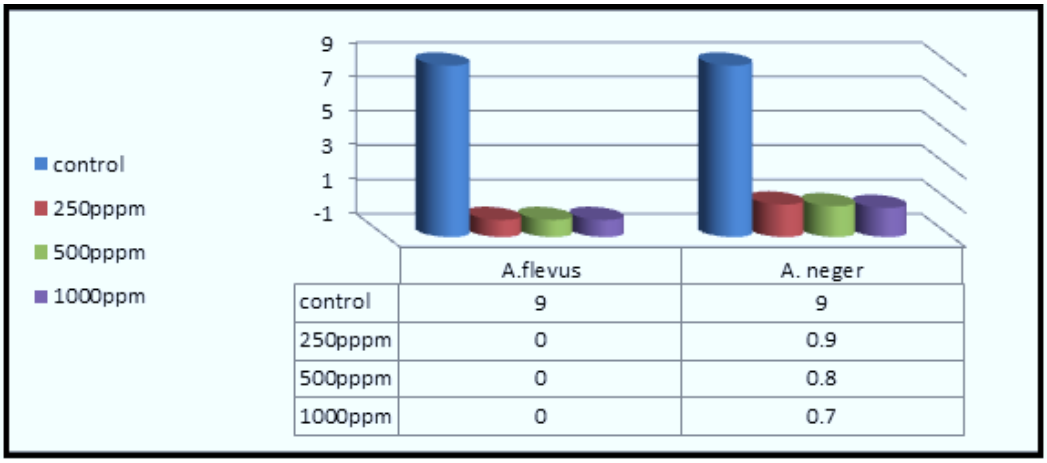

	A.flevus	A. neger
control	9	9
250pppm	0	0.9
500pppm	0	0.8
1000ppm	0	0.7

Fig.10. Showing the growth areas resulting from the biological influence of the fungus *A. flevusand A. neger* on the gold complex

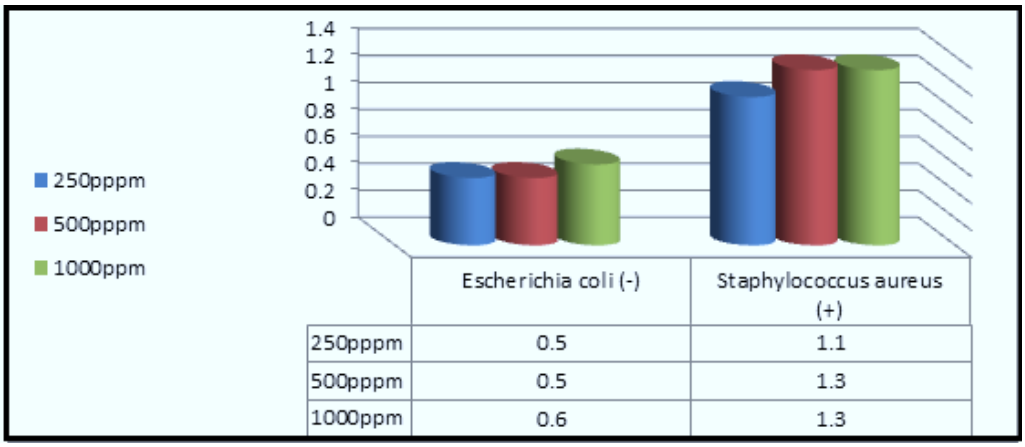

	Escherichia coli (-)	Staphylococcus aureus (+)
250pppm	0.5	1.1
500pppm	0.5	1.3
1000ppm	0.6	1.3

Fig. 11. Showing the growth areas resulting from the biological effect of *Escherichia coli* (-) and *Staphylococcus aureus* (+)on the gold complex

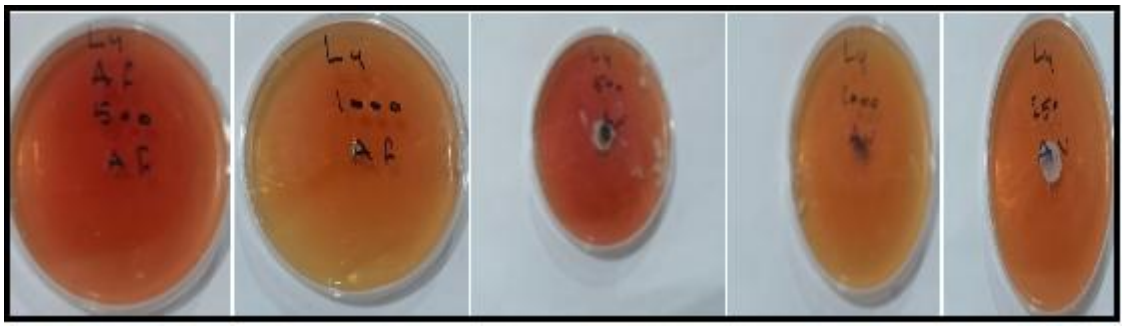

Fig. 12. Shows the effect of ligand gold complex on inhibition of *Aspergillus neger* and *Aspergillus flavus*

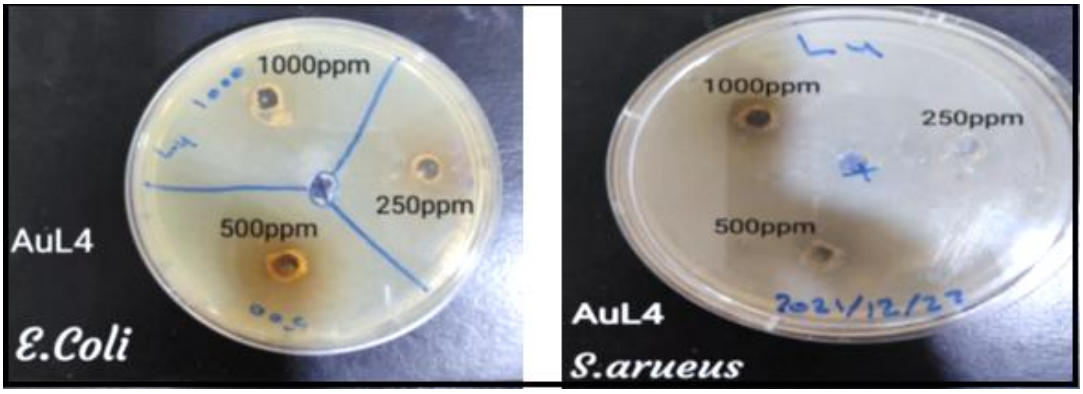

Fig. 13. Shows the effect of gold (III) complexes of ligand at different concentrations in inhibiting the two types of bacteria Escherichia coli and Staphylococcus aureus under study

3.11 Investigation of the Antibacterial Activity of Gold Complex Prepared with Ligand

Two types of pathogenic bacteria isolated from human disease cases were chosen: (Staphylococcus aureus) representing Gram positive bacteria and (Escherichia coli) representing Gram negative bacteria. There were three concentrations used. Under the same conditions, are ppm(250,500,1000) in DMSO solvent., According to the findings of this study, the inhibitory activity of the prepared metal complex against gram-negative bacteria is lower than that of gram-positive bacteria. The reason for this is that each bacterial cell is surrounded by a double membrane. Gram-negative bacteria have both an outer and an inner membrane. Show Fig. 11.

4. CONCLUSIONS

The effect of biological screening of the gold complex on human colon cancer cell line HT- 29 was investigated. The gold complex was observed to have the highest inhibitory effect.

COMPETING INTERESTS

Authors have declared that no competing interests exist.

REFERENCES

1. Kostko O, Xu B, Ahmed M. Local electronic structure of histidine in aqueous solution. Physical Chemistry Chemical Physics. 20212; 3(14):8847-8853.
2. Li S, Hong M. Protonation, tautomerization, and rotameric structure of histidine: A comprehensive study by magic-angle-spinning solid-state NMR. Journal of the American Chemical Society. 2011;133(5): 1534-1544.
3. Gopalakrishnan AK, Angamaly SA, Velayudhan MP. An Insight into the Biological Properties of Imidazole- Based Schiff Bases: A Review. Chemistry Select. 2021;6(40):10918-10947.
4. Rustandi RR. Polysorbate 80 and histidine quantitativeanalysis by NMR in the presence of virus- like particles. Electrophoresis; 2022.
5. El- Wakiel N. Nano- sized metal complexes of azoL- histidine: Synthesis, characterization and their application for catalyticoxidation of 2- amino phenol. Applied Organometallic Chemistry. 2018;32(4):e4229.
6. Ahmad S, RAbie S, Alaa M. American Journal of Analytical Chemistry. 2016;7:233–245.

7. Al-Faris ARI, Alkoofee WMS. Cobalt (II) and nickel (II) complexes with Schiff base ligand derived from 4-amino antipyrine: Synthesis, spectral, characterization and thermal studies. InternationalJournal of Engineering & Technology. 2018;7(4.37):198-201.
8. Ahmad K, Naseem HA, Parveen S, Shah SSA, Shaheen S, Ashfaq A, Ashfaq M. Synthesis and spectroscopic characterization of medicinal azo derivatives and metal complexes ofIndandion. Journal of Molecular Structure. 2019;1198: 126885.
9. Gaffer HE, Moustafa MG, Fahmy HM. Journal of Applied sciences Research. 2013;9(6):4059–4067.
10. Zechel S, Hager MD, Priemel T, Harrington MJ. Healing through histidine: Bioinspired pathways to self-healing polymersvia imidazole–metal coordination. Biomimetics. 2019;4(1):20.
11. Farmanulla K, Shafiullah K, Ali A, Wasim A, Zia-Ul-Haq, Zakir K. American Eurasian J. Agric. & Environ. Sci. 2015;15(2):216–219.
12. Raheem T, AbidAllah M, Huda A. Journal of Al-NahrainUniversity Science. 2014;17(4):51–58.
13. Al-Hamdani AAS, BALKHI A, Falah A, Shaker SA. New Azo-Schiff base derived with Ni (II), Co (II), Cu (II), Pd (II) and Pt (II) Complexes: Preparation, spectroscopic investigation, structuralstudies and biological activity. Journal of the Chilean ChemicalSociety. 2015;60(1):2774-2785.
14. Nagham Mahmood Aljamali, Nemah Sahib Muhammed. Chemo - Spectral and Biological Studying of New Ligands., Research Journal of Pharmaceutical, Biological and Chemical Sciences. RJPBCS. 2017;8(3):674.
15. Liao SM, Du QS, Meng JZ, Pang ZW, Huang RB. The multiple roles of histidine in protein interactions. ChemistryCentral Journal. 2013;7(1):1-12.
16. Abdul Gabar Abdul Maged, Amina A Fayad. Synthesis And Spectroscopic Characterization Of New Heterocyclic Compounds Derivatied From 1-(4-Aminophenyl) Ethan-1-Oneoxime As A Starting Material With Evaluate Their Biological Activity., Biochem. Cell. Arch. 2020;20(2):5211-5222.
Available:https://connectjournals.com/03896.2020.20.5211
17. Nagham Mahmood Aljamali. Synthesis of Antifungal Chemical Compounds from Fluconazole with (Pharma-Chemical) Studying., Research Journal of Pharmaceutical, Biological and Chemical Sciences. 2017;8(3): 564 -573.
18. Nagham Mahmood Aljamali, Jawad S. Preparation, Spectral Depiction, Thermal Study, and Antifungal Assay of (Formazane - Mefenamic acid)- Derivatives., Egyptian Journal of Chemistry. 2022;411(65).
DOI: 10.21608/EJCHEM.2021.88727.4266
19. Kargar H, Aghaei-Meybodi F, Elahifard MR, Tahir MN, Ashfaq M, Munawar KS. Some new Cu (II) complexes containingO, N-donor Schiff base ligands derived from 4-aminoantipyrine: Synthesis, characterization, crystal structure and substitution effect onantimicrobial activity. Journal of Coordination Chemistry. 2021;74(9-10):1534-1549.
20. Mhand K, Saden Ab, Nour Alrazzaka, Nagham Mahmood Aljamali. Synthesis, Characterization and Biological activity study for new hybridpolymers by grafting 1,3,4-triazole and 1,2,4-oxadiazle moieties ontopolyvinyl chloride., Egyptian Journal of Chemistry. 2021;64(3):1273–1283.
DOI: 10.21608/EJCHEM.2021.27879.2584
21. Vidyavathi GT, Kumar BV, Raghu AV, Aravinda T, Hani U, Murthy HA, Shridhar AH. Punica granatum pericarpextract catalyzed green chemistry approach for synthesizing novel ligandand its metal (II) complexes: Molecular docking/DNAinteractions. Journal of Molecular Structure. 2022;1249:131656.
22. Rajaa Abdul Ameer Ghafil, Nor A Alrab, Nagham Mahmood Aljamali. Synthesis of Triazole Derivatives via Multi Components Reaction and Studying of (Organic Depiction, Chromatographic Behavior, Chem-Physical Properties)., Egyptian Journal of Chemistry. 2020;63(11):4163-4174.
DOI: 10.21608/EJCHEM.2020.23541.2399
23. Ahmed IS, Moustafa MM, MMA EI Aziz. Spectrochimical Acta part A;Molecular and Biomolecular Spectroscopy. 2011;78(5):1429–1436.
24. Shiju C, Arish D, Kumaresan S. Novel water soluble Schiff base metal complexes: Synthesis, characterization, antimicrobial-,DNA cleavage, and anticancer activity. Journal of Molecular Structure. 2020;1221: 128770.
25. Wu UQ, Wang X, Wu P, Sai D, King L, RB, .Zhao J. Structure Evolution of Transition Metal-doped GoldClusters M@ Au12 (M= 3d–5d): Across the Periodic Table. The Journal of Physical Chemistry C. 2020;124(13):7449-745.
26. Benhassine A, Chouiter MI, Ali MK, Kacem-Chaouche N, Merazig H, et al. New Cd (II) complexderived from (1-methylimidazol-2-yl) methanol: Synthesis, crystalstructure, spectroscopic study, DFT and TD-DFT

calculations, antimicrobial activity and free-radical scavenging capacity. Journal of Molecular Structure. 2022;1257:132583.

27. Aparna J, Prabha Pillai, Ampili M. Antibacterial activity of *Clerodendrum infortunatum* L. and *Vanda spathulata* (L.) Spreng. AGAINST *Escherichia coli* AND Klebsiella sp., Uttar Pradesh Journal of Zoolog. 2021;42(24):637-644.
28. Sudha Mattigatti, Kailas Datkhile. Synthesis, characterization and application of green synthesized ag nps in endodontic therapy to reduce microbial biofilm. Uttar Pradesh Journal of Zoology. 2021;42(12):25-30.